

**Optimization of the baseline and the parent muon energy for a low energy neutrino factory**Amol Dighe,<sup>1,\*</sup> Srubabati Goswami,<sup>2,†</sup> and Shamayita Ray<sup>3,‡</sup><sup>1</sup>*Tata Institute of Fundamental Research, Homi Bhabha Road, Colaba, Mumbai 400005, India*<sup>2</sup>*Physical Research Laboratory, Navrangpura, Ahmedabad 380009, India*<sup>3</sup>*Laboratory for Elementary-Particle Physics, Cornell University, Ithaca, New York 14853, USA*

(Received 22 November 2011; published 2 October 2012)

We discuss the optimal setup for a low energy neutrino factory in order to achieve a  $5\sigma$  discovery of a nonzero mixing angle  $\theta_{13}$ , a nonzero  $CP$  phase  $\delta_{CP}$ , and the mass hierarchy. We explore parent muon energies in the range 5–16 GeV, and baselines in the range 500–5000 km. We present the results in terms of the reach in  $\sin^2\theta_{13}$ , emphasizing the dependence of the optimal baseline on the true value of  $\delta_{CP}$ . We show that the sensitivity of a given setup typically increases with parent muon energy, reaching saturation for higher energies. The saturation energy is larger for longer baselines; we present an estimate of this dependence. In the light of the recent indications of a large  $\theta_{13}$ , we also determine how these preferences would change if indeed a large  $\theta_{13}$  is confirmed. In such a case, the baselines  $\sim 2500$  km ( $\sim 1500$  km) may be expected to lead to hierarchy determination ( $\delta_{CP}$  discovery) with the minimum exposure.

DOI: [10.1103/PhysRevD.86.073001](https://doi.org/10.1103/PhysRevD.86.073001)

PACS numbers: 14.60.Pq

**I. INTRODUCTION**

While the indications of neutrino oscillations first came from the solar and atmospheric neutrino data, the observations from terrestrial experiments have helped provide a firm footing to our knowledge of neutrino masses and mixing. The data from all the neutrino oscillation experiments have established that there are two independent mass squared differences  $|\Delta m_{31}^2| \approx 2.35 \times 10^{-3} \text{ eV}^2$  and  $\Delta m_{21}^2 \approx 7.58 \times 10^{-5} \text{ eV}^2$ , as well as two large mixing angles  $\sin^2\theta_{23} \approx 0.42$  and  $\sin^2\theta_{12} \approx 0.306$  [1,2]. The third mixing angle  $\theta_{13}$  is small: at the  $3\sigma$  level we have an upper bound  $\sin^2\theta_{13} < 0.044$  [1] (0.035 [2]). Recent indications of a nonzero  $\theta_{13}$  have been obtained at the T2K [3] and MINOS [4] experiments, and now the global fits that incorporate these new data give a nonzero  $\theta_{13}$  at  $\sim 3\sigma$ . However, the precise value of the  $\theta_{13}$  best fit point as well as the significance for  $\theta_{13} > 0$  still depend on assumptions on the analysis of data from reactor experiments [2]. (The more recent results from the Daya Bay [5] and RENO [6] experiments, which were announced while this paper was under review, claim more than  $5\sigma$  discovery of a nonzero  $\theta_{13}$ . While our analysis has been done assuming that the value of  $\theta_{13}$  is still unknown, the implication of such a large  $\theta_{13}$  will be discussed towards the end of the paper).

The immediate goals for neutrino oscillation experiments are the measurements of (i) the mixing angle  $\theta_{13}$ , (ii) the  $CP$  violating phase  $\delta_{CP}$ , and (iii) the sign of  $\Delta m_{31}^2$ , also known as the mass hierarchy. These three quantities, along with the precision measurements of the already known ones, are necessary in order to complete our knowledge of the neutrino mass spectrum.

Among the three quantities mentioned above,  $\theta_{13}$  is the most important since the determination of the other two depends crucially on the value of this parameter. If  $\theta_{13} = 0$ , the  $CP$  phase is an unphysical quantity, while the determination of mass hierarchy, though possible in principle [7], becomes extremely challenging. If  $\sin^2 2\theta_{13} \gtrsim 0.01$ , its measurement will be within the reach of accelerator experiments like T2K, MINOS, or NO $\nu$ A that use conventional hadron beams for certain  $\delta_{CP}$  values. Indeed the recent results [3,4] indicate that such a measurement may soon be possible. If on the other hand the  $\nu_\mu \rightarrow \nu_e$  signals observed here are background or statistical fluctuations, then  $\theta_{13}$  may be even smaller. Reactor experiments, Double CHOOZ, Reno, and Daya-Bay may probe this angle as long as  $\sin^2 2\theta_{13} \gtrsim 0.033$ , 0.018, and 0.007, respectively [8], independent of the value of  $\delta_{CP}$ . (The Daya Bay [5] and RENO [6] experiments already claim the measurement of this angle to more than  $5\sigma$ , as mentioned earlier).

The most efficient way of determining mass hierarchy is the observation of the difference in Earth matter effects for the two hierarchies, which is possible if  $\theta_{13}$  is sufficiently large. Future atmospheric neutrino experiments can achieve this task for  $\sin^2 2\theta_{13} \sim 0.04$  at 95% C.L. [9]. For T2K and NO $\nu$ A, the sensitivity to hierarchy is possible for  $\sin^2 2\theta_{13} > 0.02$  at 90% C.L., albeit only for limited range of values of  $\delta_{CP}$  [10].

The measurement of  $\delta_{CP}$  is perhaps the most difficult of the three. Not only does it need a substantial value of  $\theta_{13}$ , the value of  $\delta_{CP}$  itself needs to be sufficiently different from zero for a positive signal of  $CP$  violation. Planned superbeam experiments, which would use highly intense conventional beams, have a limited sensitivity to  $\delta_{CP}$  at 90% C.L. and almost no sensitivity at  $3\sigma$  [10].

While the technology for the conventional beams is well established, the beam contamination inherent in

\*amol@theory.tifr.res.in

†sruba@prl.res.in

‡sr643@cornell.edu

such beams does not allow measurements accurate to more than a percent level. On the other hand, neutrino production from the decays of muons that are accelerated and stored in a ring (“neutrino factory”), combined with detectors that can identify the charge of leptons produced from the neutrino interactions, has the potential of measuring the quantities of interest even for much smaller  $\theta_{13}$  values. Even if the conventional beams succeed in a measurement, it is important to confirm such a measurement with another type of source, just like the measurements from solar and atmospheric experiments were later confirmed and established by terrestrial neutrino experiments. A neutrino factory is thus a discovery machine in the worst-case scenario (measurements beyond the reach of conventional beams) and a precision machine in favorable scenarios.

In a neutrino factory, accelerated muons are allowed to decay in the long straight sections of a storage ring, resulting in a strong collimated beam. A  $\mu^+$  beam decays to give  $\bar{\nu}_\mu$  and  $\nu_e$ . Oscillations of the  $\nu_e$  to  $\nu_\mu$  produce a  $\mu^-$  in the detector giving the so-called “wrong sign” muon signal, whereas the unoscillated  $\bar{\nu}_\mu$  produce the “right sign” or “same sign” muon signal of  $\mu^+$ . A detector with a charge identification capability can identify the two different types of signals separately, allowing the determination of  $P_{e\mu} \equiv P(\nu_e \rightarrow \nu_\mu)$  and  $\bar{P}_{\mu\mu} \equiv P(\bar{\nu}_\mu \rightarrow \bar{\nu}_\mu)$ . A  $\mu^-$  beam would similarly lead to the measurements of  $\bar{P}_{e\rightarrow\mu} \equiv P(\bar{\nu}_e \rightarrow \bar{\nu}_\mu)$  and  $P_{\mu\mu} \equiv P(\nu_\mu \rightarrow \nu_\mu)$ . While the sensitivity stems mainly from the wrong sign muon signal due to the appearance channels  $\nu_e \rightarrow \nu_\mu$  and  $\bar{\nu}_e \rightarrow \bar{\nu}_\mu$ , the disappearance channels  $\nu_\mu \rightarrow \nu_\mu$  and  $\bar{\nu}_\mu \rightarrow \bar{\nu}_\mu$  also contribute because of the large statistics available in these channels. The sensitivity of a neutrino factory may be up to  $\sin^2 2\theta_{13}$  as low as  $\sim 10^{-4}$  [11].

Since the appearance probability  $P_{e\mu}$  depends on all the three hitherto unknown quantities, the channel  $\nu_e \rightarrow \nu_\mu$  in principle contains information on all of them, and hence it has been acclaimed as the golden channel. However this advantage is masked by the fact that the value of  $\delta_{CP}$  is completely unknown. This gives rise to degenerate solutions making the unambiguous determination of the oscillation parameters an uphill task. An elegant solution was provided by observing that at the distance  $\sim 7500$  km, the golden channel probability  $P_{e\mu}$  becomes independent of the  $CP$  violating phase irrespective of energy, hierarchy, and oscillation parameters [12]. This baseline is the so-called “magic” baseline. A neutrino factory is considered most suitable for a magic baseline experiment because of the large flux and the small beam background.

Of course since the oscillation probability at the magic baseline is independent of the  $CP$  phase, there is no sensitivity to  $\delta_{CP}$ . Therefore though the magic baseline experiment is suitable for determination of hierarchy and  $\theta_{13}$ , one has to consider other shorter baselines for the  $\delta_{CP}$  determination. Detailed energy-baseline optimization studies by

the IDS-NF group propose two magnetized iron neutrino detectors (MIND), one at a distance of 4000 km and another at the distance of 7500 km, with a muon energy of 25 GeV [13]. However this requires high acceleration of the muons, and one has to contend with the  $1/r^2$  falloff of the flux.

In the recent past many authors have investigated the prospect of having a neutrino factory of much lower energy (4–10 GeV), and hence a shorter baseline. This was termed as the low energy neutrino factory (LENF) [14,15]. The preferred detectors at these low energies are the magnetized totally active scintillator detectors (TASD) or liquid argon detectors that can detect muon change efficiently. Recently the MIND-type detectors for LENF were also considered [16]. Nonmagnetic detectors for LENF have been considered in Ref. [17].

The most discussed baseline in the context of LENF is the DUSEL baseline of 1300 km. However, recently it was pointed out in Ref. [18] that the baseline  $\sim 2540$  km has a special property that in the inverted hierarchy (IH) the golden channel probability  $P_{e\mu}$  is independent of the  $CP$  phase around 3.3 GeV, and hence it can be used for an efficient determination of hierarchy using the  $\nu_\mu \rightarrow \nu_e$  channel in superbeams. In a subsequent Letter [19], we showed that for the same baseline, the probability  $P_{e\mu}$  in the normal hierarchy (NH) also becomes independent of the  $CP$  phase at 1.9 GeV. Therefore we termed this as the “bimagic” baseline and the energies as the magic energies. We also observed that away from the magic energies, the probabilities still depend on  $\delta_{CP}$ . Therefore an experiment at this baseline would be sensitive to all the three parameters if one uses a broadband neutrino beam from 1–4 GeV as can be obtained from a 5 GeV neutrino factory. A noteworthy point is that the distance 2540 km, which was motivated purely from physics considerations in Refs. [18,19], happens to be close to the Brookhaven-Homestake [20] and CERN-Pyhäsalmi [21] baselines.<sup>1</sup>

We note that the LENF was initially motivated to study precision neutrino properties at large  $\theta_{13}$ . Therefore, with the current indication that  $\theta_{13}$  is indeed large, an exploration of the potential of a LENF is worthwhile and timely. Since the neutrino-factory technology is still not well established, the time scale at which these experiments will start is comparatively larger, and therefore its aim should be correspondingly higher—like the measurements of the above quantities of interest to  $5\sigma$ . This is particularly true for a quantity like the mass hierarchy, which is a binary measurement. A large  $\theta_{13}$  is also conducive for a measurement of  $\delta_{CP}$  and it is likely that this aspect may play a decisive role in ascertaining which is the optimal baseline and energy. Of course if  $\theta_{13}$  happens to be smaller then it needs to be explored what is the optimum baseline

<sup>1</sup>Potential of baselines close to 2540 km have been studied in Ref. [22] in the context of superbeams.

and energy for determination of the all the three unknowns: mass hierarchy,  $\theta_{13}$ , and  $\delta_{CP}$ .

In general, optimization is a complex numerical problem. The parameters involved are energy, baseline, as well as the true values of the oscillation parameters. There is also the issue of the optimization with respect to the detector. The dependence of probabilities on the true values of  $\theta_{13}$ ,  $\delta_{CP}$ , and  $\Delta m_{31}^2$  is beyond the experimental control, so the reach of an experiment has to be assessed in the worst-case scenario as far as the values of the mixing parameters are concerned. As we shall show further in this paper, the lack of knowledge of true  $\delta_{CP}$  makes it extremely difficult to zero in on a particular baseline as “the optimal baseline” using the so-called green-field approach, where one determines the optimal baseline by a numerical scan of the relevant parameter space.

Optimization studies in the context of low energy neutrino factories have been carried out recently in Ref. [16] in the context of a MIND. In this paper we consider a detector that is a TASD. Apart from this, one of the major differences in their analysis and ours is that they present the sensitivity plots in terms of “fraction of  $\delta_{CP}$ ,” whereas our results are presented for all  $\delta_{CP}$  values in the range  $[0 - 2\pi]$  and our plots reveal the specific range of values of  $\delta_{CP}$  for which a given baseline is sensitive to a particular quantity.

The plan of the paper goes as follows. In Sec. II we discuss the physics of oscillation probabilities giving us the bimagic condition and the deviations from this condition in the nearby baselines. In Sec. III we discuss the experimental setup and the details of the numerical simulation. We present the results for the baseline optimization in Sec. IV and those for the muon energy optimization in Sec. V. The dependence on the true values of  $\delta_{CP}$  and  $|\Delta m_{31}^2|$  is shown by bands obtained by varying these parameters over their currently allowed ranges. The estimation of an optimal muon energy, given a baseline, is outlined in Sec. VI with a simple approximation. In Sec. VII we discuss the implications of a large measured  $\theta_{13}$  value for the optimization. In Sec. VIII we summarize our results and comment on future prospects.

## II. MAGIC AND BIMAGIC BASELINES

Certain properties of the neutrino flavor conversion probability  $P_{e\mu}$  can be useful for an analytical understanding of why certain baselines or parent muon energies should work better than the others. While these have been pointed out earlier [18,19,23], we expound on them here in detail, bringing out some of their most important features.

In general the  $P_{e\mu}$  oscillation probability can be written as [23]

$$P_{e\mu} = |\cos\theta_{23}A_S e^{i\delta_{CP}} + \sin\theta_{23}A_A|^2, \quad (1)$$

where  $A_S$  is the “solar” amplitude that depends on the solar parameters  $\Delta m_{21}^2$  and  $\theta_{12}$ , and  $A_A$  is the

“atmospheric” amplitude which depends on  $\Delta m_{31}^2$  and  $\theta_{13}$ . From the above expression it is evident that the  $CP$  violation in neutrino oscillation arises from the interference effects of these two amplitudes. In matter of constant density, the oscillation probability  $P_{\nu_e \rightarrow \nu_\mu}$  can be expanded keeping terms up to second order in the small parameters  $\alpha \equiv \Delta m_{21}^2 / \Delta m_{31}^2$  and  $s_{13}$  as [24]

$$P_{e\mu} = 4s_{13}^2 s_{23}^2 \frac{\sin^2[(1 - \hat{A})\Delta]}{(1 - \hat{A})^2} + \alpha^2 \sin^2 2\theta_{12} c_{23}^2 \frac{\sin^2 \hat{A}\Delta}{\hat{A}^2} + 2\alpha s_{13} \sin 2\theta_{12} \sin 2\theta_{23} \cos(\Delta - \delta_{CP}) \times \frac{\sin \hat{A}\Delta}{\hat{A}} \frac{\sin[(1 - \hat{A})\Delta]}{(1 - \hat{A})}, \quad (2)$$

where  $s_{ij} \equiv \sin\theta_{ij}$ ,  $c_{ij} \equiv \cos\theta_{ij}$ . Also,

$$\hat{A} \equiv \frac{2\sqrt{2}G_F n_e E_\nu}{\Delta m_{31}^2}, \quad \Delta \equiv \frac{\Delta m_{31}^2 L}{4E_\nu}, \quad (3)$$

where  $G_F$  is the Fermi constant and  $n_e$  is the electron number density. For neutrinos, the signs of  $\hat{A}$  and  $\Delta$  are positive for normal hierarchy and negative for inverted hierarchy.  $\hat{A}$  picks up an extra negative sign for antineutrinos. The last term in Eq. (2) corresponds to the interference term from which the  $CP$  dependence of the probability originates. This term also mixes the dependence on hierarchy and  $\delta_{CP}$ , as well as the dependence on  $\theta_{13}$  and  $\delta_{CP}$ , leading to a fourfold degeneracy [25]. There is also a degeneracy between  $(\theta_{23}, \delta_{CP})$  and  $(\pi/2 - \theta_{23}, \delta_{CP})$  [26]. Together, this eightfold degeneracy makes the determination of the oscillation parameters ambiguous. It was noticed in Ref [12] that the  $CP$  dependence of the probability can be avoided if one has

$$\sin(\hat{A}\Delta) = 0, \quad (4)$$

which corresponds to the vanishing of the solar amplitude  $A_S$  and hence the interference term. As a result  $P_{e\mu}$  becomes independent of the  $CP$  phase  $\delta_{CP}$  as well as the solar parameters. This condition is obeyed at the so-called magic baseline ( $L \sim 7500$  km) for all  $E_\nu$  and for both the hierarchies.

However, the dependence on the  $CP$  phase also vanishes when the atmospheric amplitude  $A_A$  vanishes [23], which corresponds to the condition

$$\sin[(1 - \hat{A})\Delta] = 0. \quad (5)$$

However, one notes that unlike the magic baseline condition this condition depends on energy as well as hierarchy. Therefore for a particular hierarchy and a particular baseline one can find a set of magic energies where the  $CP$  dependence in the probability vanishes. If we consider IH, the condition for no  $\delta_{CP}$  sensitivity (IH-NoCP) can be written as

$$(1 + |\hat{A}|) \cdot |\Delta| = n\pi \quad (6)$$

with the integer  $n > 0$ . The magic energies are given as

$$E_{\text{magic}}^{\text{IH}} = \frac{1.27|\Delta m_{31}^2|L}{n\pi - 1.27|K|\rho L}. \quad (7)$$

Here the quantity  $K$  has been defined such that  $K\rho \equiv 2\sqrt{2}G_F n_e$ , where  $\rho \equiv \rho(L)$  denotes the average matter density for the baseline  $L$ . For a given baseline  $L$ , at these energies the probability  $P_{e\mu}$  for IH is independent of the  $CP$  phase as well as  $\theta_{13}$ , and only the  $\mathcal{O}(\alpha^2)$  term contributes. The hierarchy dependence of the magic energy can be utilized to maximize the hierarchy sensitivity by demanding that  $\sin[(1 - \hat{A})\Delta] = \pm 1$  for NH at the same time. We will refer to this condition as NH-max. With this condition, the number of events are enhanced due to the first term in Eq. (2). Also the  $CP$  dependence is retained in the NH probability. The condition for maxima in NH can be expressed as

$$(1 - |\hat{A}|) \cdot |\Delta| = (m - 1/2)\pi, \quad (8)$$

when  $m$  is any integer. This gives

$$E_{\text{max}}^{\text{NH}} = \frac{1.27|\Delta m_{31}^2|L}{(m - 1/2)\pi + 1.27|K|\rho L}. \quad (9)$$

It may be conjectured that we will have maximum hierarchy sensitivity if

$$E_{\text{magic}}^{\text{IH}} = E_{\text{max}}^{\text{NH}}. \quad (10)$$

From the condition in Eq. (10) we arrive at the baseline

$$\rho L (\text{km g/cc}) \approx (n - m + 1/2) \times 16300. \quad (11)$$

Note that the relevant  $L$  in Eq. (11) is independent of any oscillation parameters as in the case of the magic baseline. However unlike the magic baseline this condition will be satisfied only for particular values of energy, given by  $E_{\text{magic}}^{\text{IH}} = E_{\text{max}}^{\text{NH}}$ .

Alternatively if we demand no sensitivity to  $CP$  phase in NH (NH-NoCP), we get

$$(1 - |\hat{A}|) \cdot |\Delta| = n\pi, \quad (12)$$

which gives

$$E_{\text{magic}}^{\text{NH}} = \frac{1.27|\Delta m_{31}^2|L}{n\pi + 1.27|K|\rho L}, \quad (13)$$

where  $n$  is any nonzero integer. For a given baseline  $L$ , at these energies the probability  $P_{e\mu}$  for NH is independent of the  $\delta_{CP}$  as well as  $\theta_{13}$ , and  $P_{e\mu}$  becomes  $\mathcal{O}(\alpha^2)$ . The condition for maxima for IH (IH-max) gives

$$(1 + |\hat{A}|) \cdot |\Delta| = (m - 1/2)\pi, \quad (14)$$

where  $m$  is a positive integer. This gives

$$E_{\text{max}}^{\text{IH}} = \frac{1.27|\Delta m_{31}^2|L}{(m - 1/2)\pi - 1.27|K|\rho L}. \quad (15)$$

Demanding

$$E_{\text{magic}}^{\text{NH}} = E_{\text{max}}^{\text{IH}}, \quad (16)$$

we get the same equation for the baseline  $L$ , as in Eq. (11), except for an overall negative sign which can be attributed to the different regions of validity for  $n, m$ .

Figure 1 demonstrates the existence of bimagic baselines along with the corresponding magic energies for  $n, m = 1, 2, 3$ . The left panel shows the solutions for IH-NoCP and NH-max, while the right panel shows NH-NoCP and IH-max solutions. It is clear from the figure that the baseline  $L \sim 2540$  km is the shortest baseline that satisfies both the pairs of conditions simultaneously. It is not a surprise, since the equation for the baseline Eq. (11) is similar for both the pairs of conditions. This baseline is therefore termed as bimagic [19]. For the pair IH-NoCP and NH-max, the solution is obtained from Eq. (11) with  $n = m$  and an average matter density of  $\rho \sim 3.2$  g/cc. The

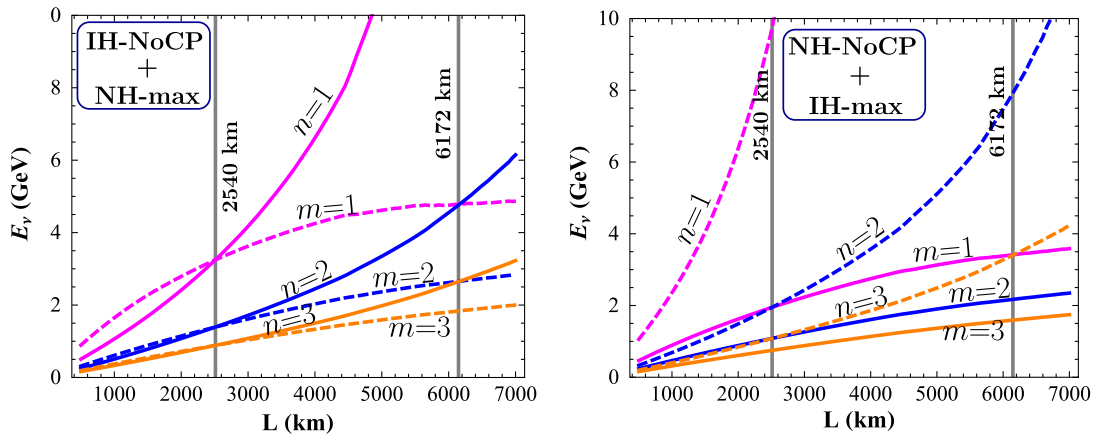


FIG. 1 (color online). Graphically solving the pair of magic conditions. Left panel:  $E_{\text{magic}}^{\text{IH}}$  (solid) and  $E_{\text{max}}^{\text{NH}}$  (dashed) as a function of  $L$  for different  $n, m$ . Right panel:  $E_{\text{magic}}^{\text{NH}}$  (solid) and  $E_{\text{max}}^{\text{IH}}$  (dashed) as a function of  $L$  for different  $n, m$ . The intersection points of the curves show the baselines and the energies at which the conditions for maximum hierarchy sensitivity are satisfied.



corresponding magic energies can be obtained from Eq. (7) or Eq. (9) to be 3.3 GeV for  $(n, m) = (1, 1)$ , 1.4 GeV for  $(n, m) = (2, 2)$ , 0.89 GeV for  $(n, m) = (3, 3)$ , and so on. Clearly the magic energies decrease with increasing  $n, m$ . Larger values of  $n, m$  are less and less practical since the flux at low energies, as well as the efficiency of detection, are typically lower. The solution for the pair NH-NoCP and IH-max is similarly obtained, the magic energies here are 1.97 GeV ( $n = 1, m = 2$ ) and 1.09 GeV ( $n = 2, m = 3$ ).

As can be seen from the figure, the baseline of 6172 km also satisfies the two pairs of conditions. With  $\rho(6172 \text{ km}) = 3.955 \text{ g/cc}$ , IH-NoCP and NH-max are satisfied for  $n - m = 1$ ; the magic energies in the relevant range are 4.8 GeV for  $(n, m) = (2, 1)$  and 2.66 GeV for  $(n, m) = (3, 2)$ . For NH-NoCP and IH-max, the interesting energy is 3.42 GeV, obtained with  $(n, m) = (1, 3)$ . This baseline therefore also deserves the title ‘‘bimagic.’’ So do the longer baselines of 8950 km and 10 690 km, which are not shown in the figure. However for the purpose of numerical optimization studies in this paper, we restrict ourselves to baselines in the range 500–5000 km, since longer baselines imply a lower flux, following the  $1/r^2$  behavior.

Even though solving the bimagic conditions given in Eqs. (10) and (16) using the Preliminary Reference Earth Model (PREM) [27] profile we get the exact values of the bimagic baselines with the magic energies, it is observed from Fig. 1 that the values of magic energy for one hierarchy and the maximum energy for the other hierarchy move away from each other rather slowly on either sides of

the intersection point, as  $L$  is varied. Moreover, currently there is  $\sim 5\%$  error on  $|\Delta m_{31}^2|$  at  $1\sigma$  as well as uncertainties associated with the density profile of the Earth. So the excellent hierarchy sensitivity of the bimagic baselines, attributed to its bimagic property, is expected to be there even if we move slightly away from these specific baselines. There already exist a few possible baselines of similar magnitudes: (i) the Brookhaven to Homestake distance is exactly 2540 km, and (ii) the CERN to Pyh asalmi (proposed site for the LENA detector) distance is 2288 km.

Figure 2 shows the probability  $P_{e\mu}$  for different baselines, for  $\sin^2\theta_{13} = 0.01$ . In this and all other plots, we have solved the exact neutrino propagation equation numerically using the PREM profile. The probability  $P_{e\mu}$  shown in Fig. 2 shows the presence of the bimagic properties for  $L \sim 2500 \text{ km}$  clearly. Around this distance, the maximum of NH appears at the same energy as the minimum of IH and vice versa, enhancing the hierarchy sensitivity. This particular feature is absent in any of the other baselines shown. When one goes to a higher baseline, the following effects occur:

- (i) The flux decreases as  $1/r^2$ .
- (ii) The amplitude of oscillations in NH increases while that in IH decreases. This would tend to increase the hierarchy sensitivity.
- (iii) The oscillation maxima of IH move faster to higher energies than that of NH, resulting in the maxima of both hierarchies coming closer in energies, which would tend to decrease the hierarchy sensitivity.

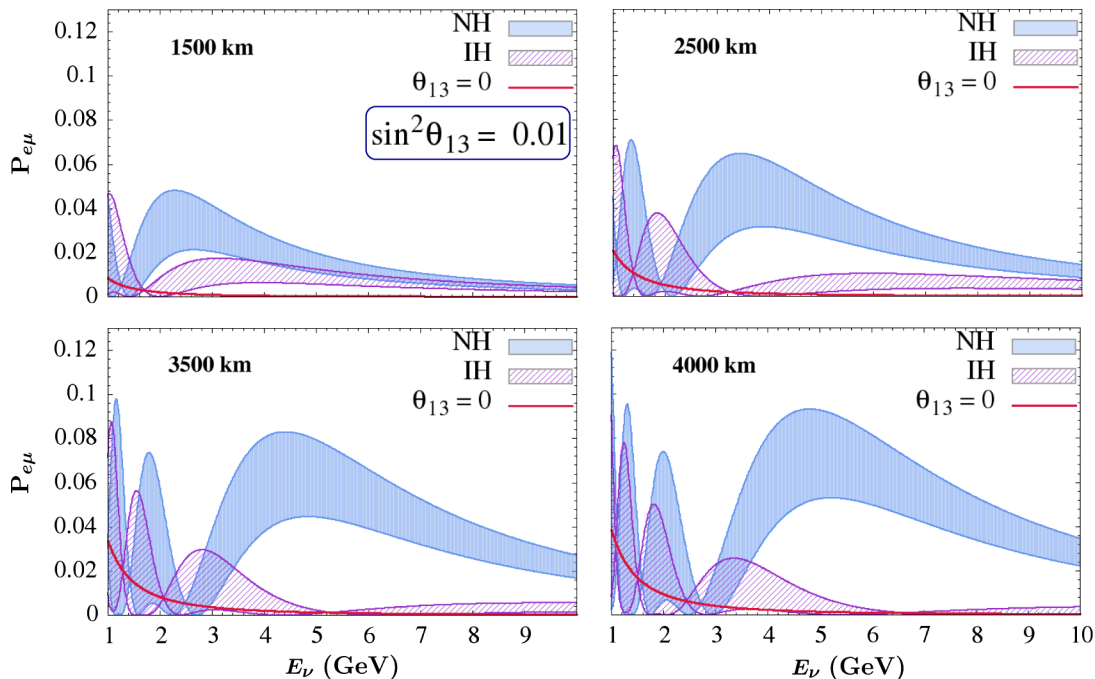


FIG. 2 (color online). Conversion probability  $P_{e\mu}$  for  $L = 1500, 2500, 3500,$  and  $4000 \text{ km}$ . The bands correspond to  $\delta_{CP} \in [0, 2\pi]$ . Other parameters are as given in Eq. (17). The red (thick) line corresponds to  $\theta_{13} = 0$ .

- (iv) At a given parent muon energy, the number of events depends on the overlap of the flux spectrum and the probability  $P_{e\mu}$ . While the flux spectrum is independent of the baseline, the major maxima in  $P_{e\mu}$  (the one at the highest energies) shift to higher energies. This results in a decrease in the overlap between the flux spectrum and  $P_{e\mu}$ , leading to a decrease in the statistics.

The net result is a subtle combination of all these effects. At the lower end of the parent muon energies  $E_\mu$ , the bimagic baseline gives the best sensitivity to hierarchy, while at higher  $E_\mu$  the optimal baseline increases.

The figure also shows the probability for  $\theta_{13} = 0$ . This is the same for both the hierarchies since in Eq. (2) at  $\theta_{13} = 0$  only the  $\mathcal{O}(\alpha^2)$  term contributes in the leading order which is independent of hierarchy. The distance of the bands from this line gives a direct estimate of  $\theta_{13}$  discovery potential for the corresponding baseline and hierarchy. The 2500 km plot in Fig. 2 suggests that  $\theta_{13}$  discovery potential is expected to be good for NH, while it may not be so good for IH as the  $P_{e\mu}$  values are lower. The same is true for the longer baselines. The conclusions get reversed for antineutrinos because of the change in sign in  $\hat{A}$  in Eq. (2). However for 1500 km, the difference between the probability values for NH and IH is not so large, and hence  $\theta_{13}$  discovery potential is expected to be similar for both the hierarchies. Of course on top of the probabilities, the cross section and the  $1/r^2$  flux dependence also contribute in determining the optimal baseline.

The sensitivity to the  $CP$  phase is related to the widths of the bands that represent the variation of the  $CP$  phase. The widths of the  $P_{e\mu}$  bands seem to increase with increasing baselines. On the other hand, the fluxes fall as  $1/r^2$ . So the optimal baseline should emerge from a compromise between these two opposing factors.

In this section we have given analytic arguments to motivate the desirable values for the baselines and neutrino energies to determine the sign of mass hierarchy, and detect nonzero values for  $\theta_{13}$  and  $\delta_{CP}$ . To choose the optimal baseline for the low energy neutrino factory, one will have to perform a complete numerical study, which we do in the next sections.

### III. DETAILS OF NUMERICAL SIMULATIONS

As the detector, we use a 25 kt T ASD with an energy threshold of 1 GeV. We choose a typical neutrino factory setup with  $5 \times 10^{21}$  useful muon decays per year, which is of the same order as in the setup considered in Refs. [15,28]. We consider the running with both the polarities, each for 2.5 years. So we have a neutrino flux consisting of  $\bar{\nu}_\mu$  and  $\nu_e$  when we consider running with  $\mu^+$ , while it becomes  $\nu_\mu$  and  $\bar{\nu}_e$  when running with negative polarity.

We assume a muon detection efficiency of 94% for energies above 1 GeV, 10% energy resolution for the whole energy range, and a background level of  $10^{-3}$  for the  $\nu_e \rightarrow \nu_\mu$  and  $\bar{\nu}_\mu \rightarrow \bar{\nu}_\mu$  channels. Detection of  $\nu_e$  or  $\bar{\nu}_e$  is not considered in this study, which seems to have a very small effect when the initial flux is as large as above [15]. A 2.5% normalization error and 0.01% calibration error, both for signal and background, have also been taken into account throughout this study. The detector characteristics have been simulated with GLOBES [29]. We also use the prescriptions for priors and marginalization inbuilt in GLOBES.

Our main goal is to find out the optimal baseline as well as the optimal parent muon energy  $E_\mu$  for that baseline. In order to optimize the baseline, we choose three representative energies for the parent muon: 5, 7.5, and 10 GeV, and vary the baseline in the range 500–5000 km. For optimizing the parent muon energy  $E_\mu$ , we choose three representative baselines: 1500, 2500, and 3500 km, and vary  $E_\mu$  in the range 2–16 GeV.

### IV. OPTIMIZATION OF THE BASELINE

In this section, we present the results of our baseline optimization for the measurement of the three “performance indicators” [16]: neutrino mass hierarchy, discovery of  $\theta_{13}$ , and  $\delta_{CP}$ . We have performed the analysis at the parent muon energies of  $E_\mu = 5, 7.5, \text{ and } 10$  GeV. The results at intermediate energies can be extrapolated from the results at these representative parent muon energies. The energy optimization will be presented in the next section.

The main sources of uncertainty in determining the reach of an experiment are the unknown values of  $\delta_{CP}$  and  $\theta_{13}$ . We therefore focus on the influence of these two quantities on our results, and keep the true values of other mixing parameters to be fixed at

$$\begin{aligned} \Delta m_{21}^2 &= 7.65 \times 10^{-5} \text{ eV}^2, & \sin^2 \theta_{12} &= 0.3, \\ |\Delta m_{31}^2| &= 2.4 \times 10^{-3} \text{ eV}^2, & \sin^2 \theta_{23} &= 0.5. \end{aligned} \quad (17)$$

We also explore the effects of varying  $|\Delta m_{31}^2|$  in its current  $3\sigma$  allowed range. In this section we present three kinds of plots:

- (i) Type-A: plots in the  $\sin^2 \theta_{13} - L$  plane for fixed true values of  $|\Delta m_{31}^2|$  and  $\delta_{CP}$  varying in the range  $[0, 2\pi]$ ,
- (ii) Type-B: plots in the  $\delta_{CP} - L$  plane for fixed true values of  $\sin^2 \theta_{13}$  and  $|\Delta m_{31}^2|$ ,
- (iii) Type-C: plots in the  $\sin^2 \theta_{13} - L$  plane for fixed true values of  $\delta_{CP}$  and varying  $|\Delta m_{31}^2|$  in its current  $3\sigma$  range.

In the conventional plots the reach for a particular performance indicator is often given in terms of the fraction of  $\delta_{CP}$  values for which the determination of a quantity is possible. Our Type-A plots show the reach for all

possible  $\delta_{CP}$  values from which the reach even for the worst-case  $\delta_{CP}$  values may be inferred. Moreover, from the Type-B plots that show the reach for all  $\delta_{CP}$  values, one may also trivially infer the fraction of  $\delta_{CP}$  for which the quantity may be determined.

For reference, in the baseline optimization plots we also show two vertical lines, corresponding to the baselines of 2540 km, the ‘‘bimagic’’ baseline, and 1300 km, the baseline that is perhaps the most studied in the context of the LENF.

### A. Hierarchy determination

In order to optimize the baseline for the determination of hierarchy, we assume NH to be the true hierarchy and show the reach of  $\theta_{13}$  for which the wrong hierarchy (IH) can be excluded to  $5\sigma$ , as a function of the baseline. Note that the

determination of hierarchy is a binary measurement, and hence a  $5\sigma$  determination is absolutely necessary before claiming a positive identification of this quantity.

Figure 3 shows the hierarchy sensitivity with the stated experimental setup. In the top panel we present Type-A plots, where true values of  $\sin^2\theta_{13}$  are plotted along the vertical axis. True values of all other parameters, except  $\delta_{CP}$ , are set to values stated in Eq. (17). To generate the bands in this top panel,  $\delta_{CP}(\text{true})$  is varied over the complete range of  $[0, 2\pi]$ . For each set of chosen values of mixing parameters and chosen baseline,  $\chi^2_{\min}$  is obtained by marginalizing over all parameters with the wrong hierarchy. We have taken 4% error on each of  $\Delta m_{21}^2$  and  $\theta_{12}$ , and 5% on  $\theta_{23}$  and  $|\Delta m_{31}^2|$ . A 2% error has also been considered on the Earth matter profile and marginalized over.

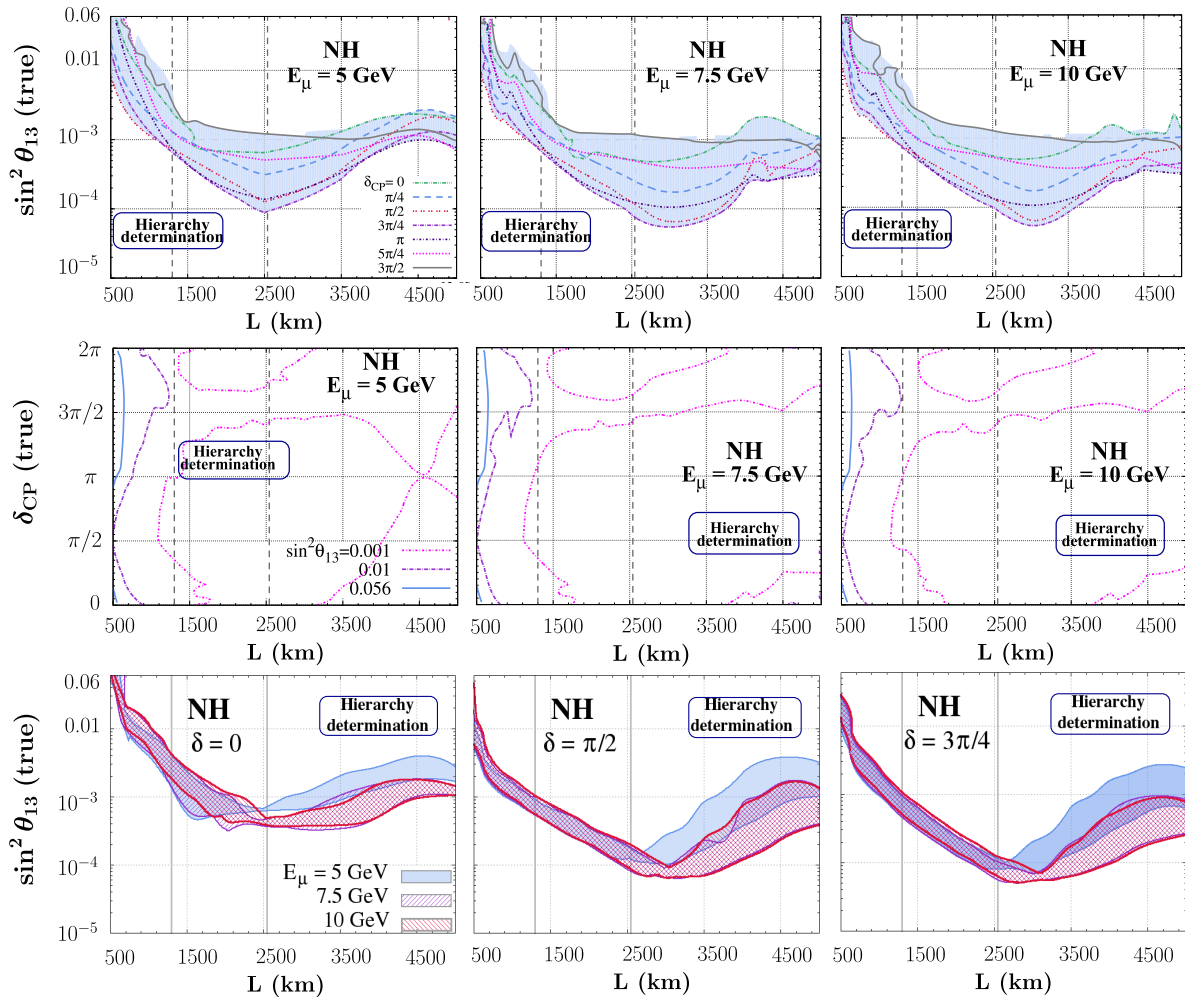


FIG. 3 (color online).  $5\sigma$  reach in hierarchy determination for fixed muon energies, as a function of baseline, assuming the true hierarchy to be NH. The top panel gives the reach in  $\sin^2\theta_{13}$ , the bands correspond to  $\delta_{CP} \in [0, 2\pi]$ . Specific values of  $\delta_{CP}$  are also shown within the band. The middle panel shows the  $5\sigma$  reach in  $\delta_{CP}$  for fixed values of  $\sin^2\theta_{13}$ . The bottom panel denotes the reach in  $\sin^2\theta_{13}$  for fixed values of  $\delta_{CP}$ . The bands correspond to the current  $3\sigma$  range of  $|\Delta m_{31}^2|$ . All the undisplayed parameters are fixed at values given in Eq. (17). The plots are generated for 2.5 years of running with each muon polarity. The two dark vertical lines correspond to the baselines of 2540 km (the bimagic baseline) and 1300 km.

The figures in the top panel of Fig. 3 show that the baseline optimization depends on the actual  $\delta_{CP}$  value as well as the parent muon energy  $E_\mu$ . The widths of the bands, which span almost an order of magnitude in  $\sin^2\theta_{13}$ , are mainly due to the variation in  $\delta_{CP}$ , while the dependence on  $E_\mu$  may be discerned from the variation across the three plots in the panel. For each baseline, the upper edge of the band gives the lowest value of  $\theta_{13}$  for which hierarchy can be determined at  $5\sigma$  in the most conservative case, i.e., irrespective of what the true value of  $\delta_{CP}$  is.

The leftmost top panel shows that for  $E_\mu = 5$  GeV, the reach of the experiment is optimal at  $L \sim 2500$  km for most of the  $\delta_{CP}$  values; however the actual reach depends strongly on the true  $\delta_{CP}$ . At the optimal baseline the reach in  $\sin^2\theta_{13}$  varies over an order of magnitude from  $\sim 10^{-4}$  to  $10^{-3}$ . The maximum reach around this baseline is for  $\delta_{CP}(\text{true}) = 3\pi/4$ , which is consistent with the analytic estimate obtained in Ref. [19]. For increasing parent muon energies, the optimal baseline typically increases. For longer baselines the maximum of NH and minimum of IH shifts to higher energies. Although the condition  $E_{\text{max}}^{\text{NH}} = E_{\text{magic}}^{\text{IH}}$  is not exactly satisfied, the broader width of the oscillation curve for higher baselines contributes to give an enhanced sensitivity. The widths of the bands in the top panel are rather conservative since they include all true values of  $\delta_{CP}$ .

In reality there is a unique true value of  $\delta_{CP}$ , which controls the reach for  $\sin^2\theta_{13}$  for a given baseline. Since this true value is unknown in the analysis it has to be kept free. In order to understand what are the specific values of  $\delta_{CP}$  for which hierarchy can be determined at a particular baseline, we also present the Type-B plots in the middle panel of Fig. 3, plots for fixed  $\theta_{13}$  values in the  $\delta_{CP} - L$  plane.

The middle-panel plot for 5 GeV muon energy shows that if  $\sin^2\theta_{13}$  is 0.056, then it is possible to determine hierarchy at  $5\sigma$  level for all values of  $\delta_{CP}$  for  $L \geq 700$  km. For  $\sin^2\theta_{13} = 0.01$ , one needs to go beyond 1200 km if  $\delta_{CP} > 3\pi/2$ . For  $\sin^2\theta_{13} = 0.001$ , there is some sensitivity to hierarchy for  $L \approx 1100$  km, but only for  $\delta_{CP}$  close to  $\pi/2$ . Hierarchy sensitivity at 1300 km for this value of  $\theta_{13}$  exists only for  $\sim 32\%$  of the possible  $\delta_{CP}$  values. The baseline that offers sensitivity to the largest range of  $\delta_{CP}$  values at such low  $\theta_{13}$  is 1800–2500 km. As we go beyond 3000 km the range of  $\delta_{CP}$  values for which hierarchy can be determined becomes much smaller for  $E_\mu = 5$  GeV. However if the energy is increased, then higher baselines can determine hierarchy for a wider range of  $\delta_{CP}$  values. One striking feature seen from these plots is that there is a small range of  $\delta_{CP}$  values around  $3\pi/2$  for which hierarchy cannot be determined by LENF for  $\sin^2\theta_{13} = 0.001$ . This can be remedied by a combination with another experiment that is sensitive to the region around  $\delta_{CP} = 3\pi/2$ .

Another uncertainty in the hierarchy sensitivity of a given experimental setup can come from  $|\Delta m_{31}^2|$ , as the

magic energies depend on it. To illustrate this dependence, we show Type-C plots in the bottom panel of Fig. 3 for three fixed  $\delta_{CP}$  (true) values:  $\delta_{CP}(\text{true}) = 0$  (no CPV),  $\pi/2$  (maximum CPV), and  $3\pi/4$  (intermediate CPV). The true value of  $|\Delta m_{31}^2|$  is varied over its  $3\sigma$  range, giving rise to bands with a finite width. Each plot shows the bands for the three representative  $E_\mu$  values, stated before.

The widths of the bands in the bottom panel of Fig. 3 show that the dependence of hierarchy sensitivity on  $|\Delta m_{31}^2|$  is much smaller compared to that on the true value of  $\delta_{CP}$ . From the leftmost figure in the panel, we see that for no CPV, the best hierarchy sensitivity is obtained in a rather broad baseline regime 1500–3500 km, though for the worst-case values of  $|\Delta m_{31}^2|$ , the range around 2500 km is preferred, where the error due to  $|\Delta m_{31}^2|$  is also small. If CPV is maximum ( $\delta_{CP} = \pi/2$ , central panel) or has the chosen value of  $3\pi/4$  (right panel), the maximum hierarchy sensitivity is for a comparatively narrower, but still wide, baseline range  $\sim 2300$ –3500 km, near the bimagic baseline. At the worst-case values of  $|\Delta m_{31}^2|$ , a baseline  $\sim 2500$  km is preferred for  $E_\mu = 5$  GeV, while it shifts to  $\sim 3000$  km for higher  $E_\mu$  values. Among the three  $\delta_{CP}$  values considered, the sensitivity to hierarchy is observed to be the worst for the scenario with no CPV; however, as can be seen from the top panel, different values of  $\delta_{CP}$  are the worse-case scenarios for different baselines. As the parent muon energy increases, the optimal baseline shifts to higher values as expected. The sensitivity is seen to increase when  $E_\mu$  increases from 5 to 7.5 GeV, but thereafter it seems to saturate. This feature will be discussed in detail in the next sections.

Our results in this section clearly indicate that if hierarchy sensitivity is considered as the performance indicator, and if  $\sin^2\theta_{13} \lesssim 0.001$  and  $E_\mu = 5$  GeV, then the hierarchy can be determined for a larger ( $\sim 86\%$ ) fraction of possible  $\delta_{CP}$  values at 2540 km, the bimagic baseline. This fraction increases for higher  $E_\mu$  values. For  $\sin^2\theta_{13} > 0.01$ , hierarchy determination is possible for all values of  $\delta_{CP}$ , as long as  $E_\mu > 5$  GeV and  $L > 1300$  km.

## B. $\theta_{13}$ discovery

In this section, we apply the same analysis techniques as the last section to the discovery potential of  $\theta_{13}$ . Note that though a  $\sim 2.5\sigma$  evidence for nonzero  $\theta_{13}$  has recently been claimed by experiments [3,4] and the global fit to the neutrino mixing parameters [1,2], the jury is still out on this and it is quite possible that the value of  $\theta_{13}$  is much smaller. Also, since we are looking towards a long-term experiment, we should not be satisfied with a  $3\sigma$  evidence, but should try to gauge the potential of an experiment for a definitive  $5\sigma$  discovery.<sup>2</sup> Figure 4 shows the  $5\sigma$  reach for

<sup>2</sup>The implications of the recent Daya Bay [5] and RENO [6] results are discussed towards the end of the paper.



$\theta_{13}$  discovery for three different parent muon energies in terms of the three types of plots, Type-A, B, and C, as mentioned above.

The widths of the bands in the top panel show that  $\theta_{13}$  discovery potential of a baseline depends strongly on the true value of  $\delta_{CP}$ . Indeed for any baseline, the best-case and the worst-case values of  $\delta_{CP}$  make a difference of almost an order of magnitude in the corresponding reach for  $\sin^2\theta_{13}$ . Shorter baselines are seen to be generally preferred for  $\theta_{13}$  discovery, as compared to those preferred for hierarchy determination. For example, for  $E_\mu = 5$  GeV, the optimal baseline is  $\sim 800$ – $1600$  km, while for higher parent muon energies it moves to  $\sim 1500$ – $2500$  km. At all these energies, it is observed that the sensitivity is maximum when  $\delta_{CP} \approx \pi/2$ . With the worst-case values of  $\delta_{CP}$ , the optimal baseline stays near  $1500$ – $2000$  km in the whole energy range.

In the middle panel of Fig. 4 we present the Type-B plots. For  $\sin^2\theta_{13} = 0.001$ , the discovery of  $\theta_{13}$  is possible for regions outside the magenta (dashed) contour. Thus for  $L < 2100$  km,  $\theta_{13}$  can be discovered irrespective of  $\delta_{CP}$  for this value of  $\sin^2\theta_{13}$ . Higher  $\theta_{13}$  values can be discovered in the whole  $\delta_{CP} - L$  plane. For  $\sin^2\theta_{13} = 0.0001$ , the discovery of  $\theta_{13}$  is possible for the area inside the dot-dot-dashed green contours, i.e., only for shorter baselines and a limited range of  $\delta_{CP}$ . For higher baselines like  $L \sim 3000$  km,  $\theta_{13}$  discovery is possible only if  $E_\mu$  is high and  $\delta_{CP}$  has values close to  $\pi/2$  or  $7\pi/4$ . In general for such small values of  $\sin^2\theta_{13}$ , the baseline of  $\sim 1500$  km seems to have  $\theta_{13}$  sensitivity for a wider range of  $\delta_{CP}$  values.

In the bottom panel of Fig. 4, we present the Type-C plots for  $\theta_{13}$  sensitivity. It illustrates the dependence of the optimal baseline on the true value of  $\delta_{CP}$ ; while for  $\delta_{CP} = 0$  the optimal baseline seems to be  $\sim 1300$ – $1500$  km, for

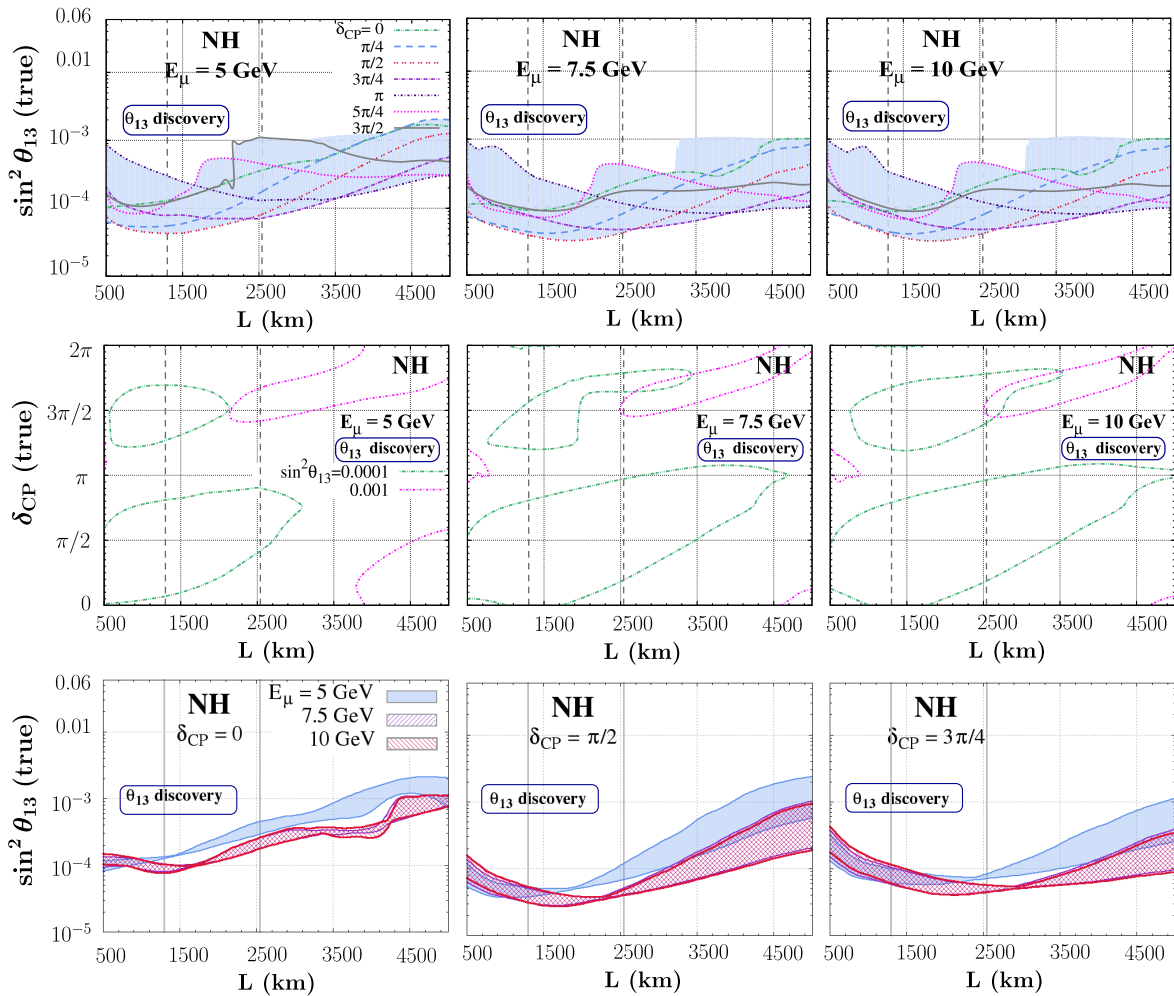


FIG. 4 (color online).  $5\sigma$  reach in  $\theta_{13}$  discovery for fixed muon energies, as a function of baseline, assuming the true hierarchy to be NH. The same conventions as in Fig. 3 are used. In the middle panel, for  $\sin^2\theta_{13} = 0.001$ , the discovery of  $\theta_{13}$  is possible for regions outside the dashed (magenta) contour. For  $\sin^2\theta_{13} = 0.0001$ , the discovery of  $\theta_{13}$  is possible for the area inside the dot-dot-dashed (green) contours.

$\delta_{CP} = \pi/2$  it is  $\sim 1500\text{--}2000$  km, and for  $\delta_{CP} = 3\pi/4$ , the most efficient baseline is  $\sim 2500$  km.

To summarize, if  $\theta_{13}$  discovery is chosen as the performance indicator, baselines in the region  $1500\text{--}2000$  km seem to work best, the actual value of the optimal baseline being dependent on the true value of  $\delta_{CP}$ . However if  $\sin^2\theta_{13} > 0.001$ , then a LENF with  $E_\mu$  in the range  $5\text{--}10$  GeV can discover  $\theta_{13}$  at  $5\sigma$  for any baseline in the range  $500\text{--}2500$  km for almost all values of true  $\delta_{CP}$ .

### C. $\delta_{CP}$ discovery

Next we move to the  $\delta_{CP}$  discovery potential in this section. The top panel of Fig. 5 shows the  $5\sigma$  reach of  $\sin^2\theta_{13}$  for  $\delta_{CP}$  discovery, given a true  $\delta_{CP}$  value. True values of all other parameters have been fixed to values mentioned in Eq. (17), while the true value of  $\delta_{CP}$  is chosen as  $\pi/4$ ,  $\pi/2$ ,  $3\pi/4$ ,  $5\pi/4$ ,  $3\pi/2$ , and  $7\pi/4$ . We do not choose  $\delta_{CP}(\text{true})$  too close to zero or  $\pi$  since the discovery potential is expected to be low. Finally  $\chi^2_{\min}$  is

obtained by marginalizing over all parameters except  $\delta_{CP}$ , for each  $\sin^2\theta_{13}(\text{true})$ . Errors on different parameters are taken to be the same as stated in Sec. IV A.

It is observed that the best-case sensitivity for  $\delta_{CP}$  is when  $\delta_{CP}$  is near  $\pi/2$ . For smaller baselines  $\delta_{CP} = 3\pi/2$  also has similar sensitivity, while between  $3500$  and  $4500$  km and for energies  $5$  and  $7.5$  GeV the sensitivity is better. It is expected that  $\delta_{CP} = \pi/2$  and  $3\pi/2$  should produce the best-case sensitivity for  $\delta_{CP}$  since it is at these values that the  $CP$  violation is maximum. Typically for all  $\delta_{CP}$  values and all parent muon energies, the baselines  $\sim 800\text{--}2000$  km seem to be the most efficient. For  $\delta_{CP} = 3\pi/4$ ,  $5\pi/4$ ,  $7\pi/4$ , on the other hand, the sensitivity is much worse. Nevertheless, baselines of  $\lesssim 2000$  km are preferred.

The middle panel of Fig. 5 gives the sensitivity to  $\delta_{CP}$  as a function of baseline for three fixed values of  $\sin^2\theta_{13}$  which are  $0.056$ ,  $0.01$ , and  $0.001$  and three values of energy  $E_\mu = 5, 7.5, \text{ and } 10$  GeV. These are representative values and the results for intermediate values of  $\sin^2\theta_{13}$  can be

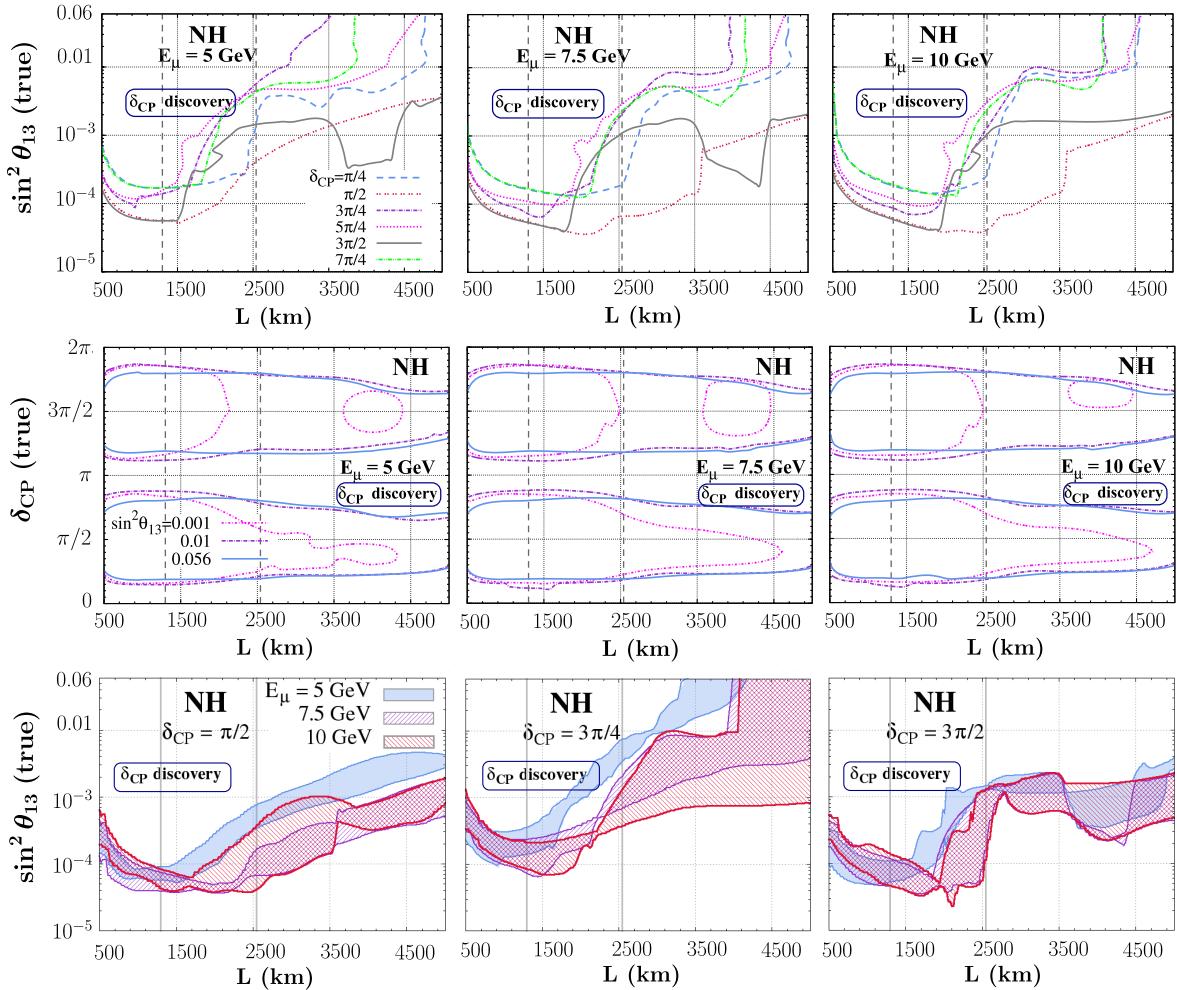


FIG. 5 (color online).  $5\sigma$  reach in  $\delta_{CP}$  discovery for fixed muon energies, as a function of baseline, assuming the true hierarchy to be NH. The same conventions as in Fig. 3 are used. In the middle panel,  $\delta_{CP}$  discovery is possible for enclosed regions that do not include  $\delta_{CP} = 0$  or  $\pi$ .

adjudged. The figure shows that for  $\sin^2\theta_{13} > 0.01$ , if  $\delta_{CP}$  lies in the ranges  $(0.3-0.7)\pi$  or  $(1.3-1.7)\pi$ , it is possible to discover nonzero  $\delta_{CP}$  at  $5\sigma$  for all baselines and all energies considered here, though smaller baselines are a bit more efficient. For lower  $\theta_{13}$  values, only shorter baselines,  $L \lesssim 2000$  km, have the possibility of detection of  $CP$  violation for most of the  $\delta_{CP}$  range. Longer baselines need higher muon energies and specific  $\delta_{CP}$  values near  $\pi/2$ ,  $3\pi/2$  in order to achieve the task.

The bottom panel of Fig. 5 gives the Type-C plots for  $\delta_{CP}$  discovery for three fixed values:  $\pi/2$ ,  $3\pi/4$ ,  $3\pi/2$ . This figure corroborates that the sensitivity to  $CP$  violation discovery is highest for  $\delta_{CP} = 3\pi/2$ . The distance at which the best sensitivity is reached is  $\sim 1700$  km (for  $\delta_{CP} = \pi/2$ ) and  $\sim 2100$  km (for  $\delta_{CP} = 3\pi/2$ ). For  $\delta_{CP} = 3\pi/4$  the range 1500–2500 km has best sensitivity. In general, the sensitivity is better at higher energies.

To summarize, the  $\delta_{CP}$  discovery potential at various baselines depends on the true  $\sin^2\theta_{13}$ . For  $\sin^2\theta_{13}$  up to 0.001,  $\delta_{CP}$  that is not too close to 0 or  $2\pi$  can be discovered at  $5\sigma$  by the LENF setup for baselines 500–2000 km. In general, lower baselines can access a wider range of  $\delta_{CP}$  values.

## V. OPTIMIZING PARENT MUON ENERGY $E_\mu$

As seen in the last section, the optimal values of the baselines depend on the parent muon energies in addition to the true values of neutrino mixing parameters. In this section, we choose three representative values for the baseline—1500, 2500, and 3500 km—and perform optimization over the parent muon energies. We use three different performance indicators as before: hierarchy determination,  $\theta_{13}$  discovery, and  $\delta_{CP}$  discovery. The parent muon energy range considered here is 2–16 GeV, covering the range of the proposed LENFs. We present only plots of Type-A, since most of the features of the energy dependence may be obtained through interpolation using the representative values  $E_\mu = 5, 7.5, \text{ and } 10$  GeV chosen in the last section.

### A. Hierarchy determination

The top panel of Fig. 6 shows the  $5\sigma$  hierarchy determination range for the three chosen benchmark baselines. For each chosen true value of  $\sin^2\theta_{13}$  and  $E_\mu$ , we obtain  $\chi_{\min}^2$  by marginalizing over all parameters assuming IH, while the true hierarchy is taken to be NH. All the parameters, except  $\delta_{CP}$ , are fixed to the values quoted in Eq. (17) and the band is generated by varying  $\delta_{CP}$  in the full range  $[0, 2\pi]$ . Errors on different parameters have been taken to be the same as described in Sec. IV A.

Similar to the case of baseline optimization in Fig. 3, the large width of the band indicates the strong dependence of hierarchy determination potential for a given experimental setup on the true value of  $\delta_{CP}$ . As far as the dependence on

$E_\mu$  is concerned, the sensitivity increases with  $E_\mu$  at low  $E_\mu$  values, and saturates at a certain value of  $E_\mu$  beyond which there is virtually no change in the sensitivity. Let us refer to this energy as the saturation energy,  $E_\mu^{\text{Sat}}$ . It is observed that  $E_\mu^{\text{Sat}}$  increases with increasing baseline, the values being  $E_\mu^{\text{Sat}} \sim 5$  GeV for 1500 km,  $E_\mu^{\text{Sat}} \sim 7$  GeV for 2500 km, and  $E_\mu^{\text{Sat}} \sim 10$  GeV for 3500 km. The sensitivity reached at  $E_\mu^{\text{Sat}}$  also increases with the baseline.

The saturation behavior indicates that one will tend to get significantly better sensitivity with increasing  $E_\mu$  and baseline till some limit, beyond which the gain may not be worth the increased acceleration required. We observe that  $E_\mu^{\text{Sat}}$  depends significantly on  $\delta_{CP}$  as well; however, this dependence is not a straightforward one. The sensitivity at a baseline of 2500 or 3500 km is always better than that at 1500 km, sometimes by up to an order of magnitude, for energies beyond  $\sim 6$  GeV. The performances at 2500 and 3500 km are comparable: the latter is marginally better, but requires higher  $E_\mu$  to achieve its full potential.

Thus if hierarchy determination is considered as the performance indicator, then a LENF can determine hierarchy for  $\sin^2\theta_{13}$  as low as 0.002 at a baseline  $L \sim 2500$  km for  $E_\mu > 5$  GeV, for any  $\delta_{CP}(\text{true})$ . If true  $\sin^2\theta_{13}$  happens to be large, then shorter baselines and smaller energies would be sufficient.

### B. $\theta_{13}$ discovery

In this section we present the result of our study of  $\theta_{13}$  discovery potential as a function of the parent muon energy  $E_\mu$  for the three benchmark baselines. The middle panel of Fig. 6 shows the  $5\sigma$  contours when  $\delta_{CP}(\text{true})$  is varied in  $[0, 2\pi]$  and also for seven chosen true values of  $\delta_{CP}$ . True values of all other parameters other than the displayed ones have been fixed to the values mentioned in Eq. (17), and  $\chi_{\min}^2$  is obtained by marginalizing over all except  $\theta_{13}$ , with the errors stated in Sec. IV A.

These figures also confirm that the discovery potential of any experimental setup depends crucially on the knowledge of  $\delta_{CP}$ . For 1500 km, the sensitivity is the best when  $\delta_{CP} \approx \pi/2$ , while for higher baselines  $\delta_{CP} \approx 3\pi/4$  has comparable or slightly better sensitivity; however the conservative reach for  $\theta_{13}$  may be up to an order of magnitude worse. Larger baselines require larger muon energies to get an equivalent sensitivity; however with such a larger  $E_\mu$ , their reach in  $\theta_{13}$  may be better.

The saturation behavior as in the case of hierarchy determination—i.e., the sensitivity increases with  $E_\mu$  till a saturation value  $E_\mu^{\text{Sat}}$ —is observed even for  $\theta_{13}$  discovery for most  $\delta_{CP}$  values.

### C. $\delta_{CP}$ discovery

The analysis of the optimal parent muon energy for  $\delta_{CP}$  discovery is carried out on the same lines as that in Sec. IV C. The plots in the bottom panel of Fig. 6 show

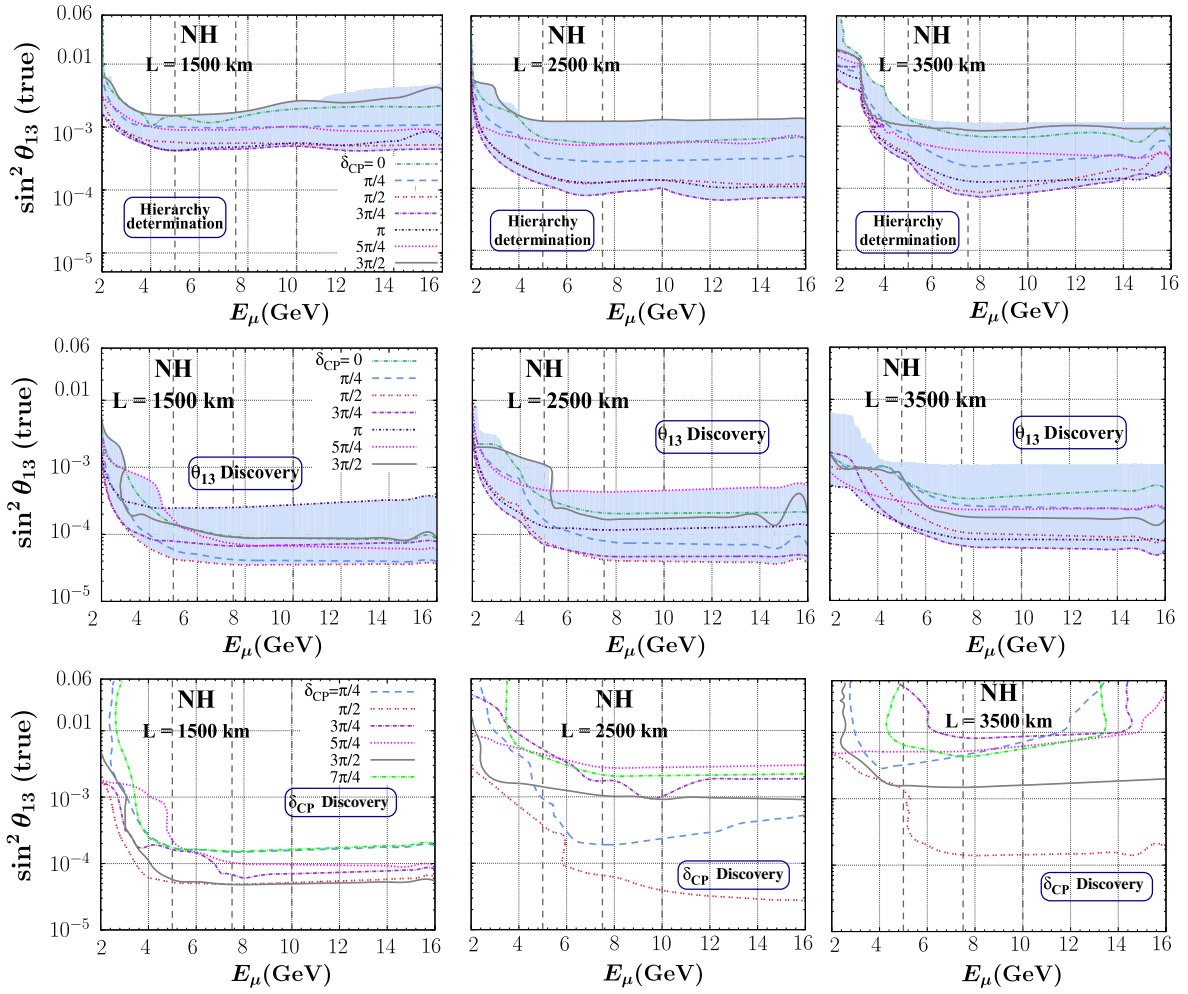


FIG. 6 (color online).  $5\sigma$  reach in  $\sin^2\theta_{13}$  for (top panel) hierarchy determination, (middle panel)  $\theta_{13}$  discovery, and (bottom panel) nonzero  $\delta_{CP}$  discovery, as a function of  $E_\mu$ , for fixed  $\delta_{CP}$  values. NH is taken as the true hierarchy. All parameters except  $\delta_{CP}$  are fixed at values quoted in Eq. (17). The exposure is taken to be 2.5 years of running with each polarity. The dark vertical lines correspond to energies 5, 7.5, and 10 GeV.

the  $5\sigma$  discovery potential contours as a function of  $E_\mu$ , for six chosen true values of  $\delta_{CP}$ , for each of the three representative baselines.

It is observed that in general the sensitivity to  $\delta_{CP}$  discovery decreases as the baseline increases. For most values of  $\delta_{CP}$  the baseline of 1500 km with  $E_\mu = 6\text{--}7.5$  GeV is seen to give the best sensitivity in Fig. 6, while for  $\delta_{CP} = \pi/2$  a baseline of 2500 km and energy  $\sim 12$  GeV seem to do better. For all the three chosen baselines better sensitivity to  $\delta_{CP}$  comes beyond  $E_\mu = 5$  GeV.

## VI. OPTIMAL PARENT MUON ENERGY FOR A GIVEN BASELINE

The two design parameters of a LENF that can in principle be controlled are the baseline and the parent muon energy that determines the neutrino fluxes at the source. Ideally one can look for the optimal combination

of both of these; however it may not always be practical. In particular, considerations behind choosing a baseline involve factors like the location suitable for an accelerator and a location where an underground laboratory for neutrino detection can be built. Apart from scientific considerations, this involves geography, economics, as well as sociology. A survey of such pairs of locations was recently carried out [16]. Given a baseline, the choice of the parent muon energy is relatively straightforward, limited mainly by technological considerations. The energy of the muon beam can then be chosen based on the optimality analysis.

As has been noticed multiple times in the previous two sections, the performance at a baseline typically increases with increasing parent muon energy  $E_\mu$  (in the LENF range) till it saturates at a particular value  $E_\mu^{\text{Sat}}$ . Given that increasing the muon energy is associated with additional costs, a desirable thing to do would be to choose the value of  $E_\mu$  at or near the value of  $E_\mu^{\text{Sat}}$ . In this section, we



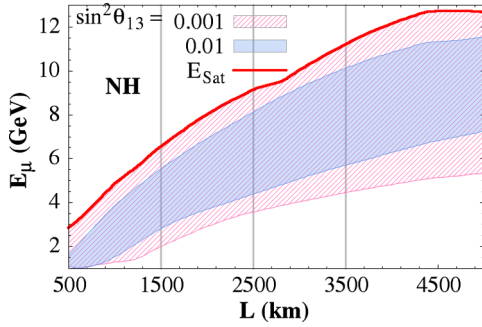


FIG. 7 (color online). The optimal value  $E_\mu^{\text{opt}}$  as a function of the baseline for normal hierarchy and with  $\sin^2\theta_{13} = 0.001$  and  $0.01$ .

obtain the  $E_\mu^{\text{Sat}}$  values for arbitrary baselines using a simple approximation. It turns out that this approximation matches the numerical  $E_\mu^{\text{Sat}}$  values observed in the previous section.

We expect that the main factor influencing the efficiency at a given energy will be the number of wrong-sign muon events. While the actual numbers will depend on the detector characteristics, we estimate this efficiency simply through the “quality factor”

$$Q \equiv \frac{\int \Phi_{\nu_e} P_{e\mu} \sigma_{\nu_\mu} dE_{\nu_e}}{\int \Phi_{\nu_e} \sigma_{\nu_\mu} dE_{\nu_e}}, \quad (18)$$

where  $\Phi_{\nu_e}$  is the flux of  $\nu_e$  at the source and  $\sigma_{\nu_\mu}$  is the total charged-current cross section of  $\nu_\mu$  at the detector. We have normalized the events to a complete  $\nu_e \rightarrow \nu_\mu$  conversion. Since the parent muon energy at the source determines the neutrino spectra at the source completely, and the baseline determines the oscillation probability completely (modulo our knowledge about the mixing parameters), the quality factor is known for a energy-baseline combination. The optimal energy  $E_\mu^{\text{opt}}$  is the one for which this quality factor is maximum. There will be a spread in  $E_\mu^{\text{opt}}$  due to the uncertainties in mixing parameters, mainly  $\theta_{13}$ ,  $|\Delta m_{31}^2|$ , and  $\delta_{CP}$ .

Figure 7 shows the  $E_\mu^{\text{opt}}$  values as functions of baseline  $L$ , for  $\sin^2\theta_{13} = 0.001, 0.01$ . The width is obtained due to variation of  $E_\mu^{\text{opt}}$  as  $|\Delta m_{31}^2|$  is varied in the current  $3\sigma$  range and  $\delta_{CP}$  in  $[0, 2\pi]$ . This gives a good estimation of what  $E_\mu$  values will be optimal corresponding to a given baseline, and can work as a rough guideline for determining the optimal range of  $E_\mu$ , once the baseline  $L$  has been determined from other considerations. Then the upper limit can be used to estimate  $E_\mu^{\text{Sat}}$  for a given baseline. Going beyond  $E_\mu^{\text{Sat}}$  would not improve the performance of the setup.

## VII. IF $\theta_{13}$ IS LARGE

The indications of a large  $\theta_{13}$  value from the experiments [3,4] and the global fit to neutrino data [1,2] is good

news for the measurements of other neutrino parameters too. In particular, it makes it easier to determine the mass hierarchy, and makes the measurement of  $\delta_{CP}$  possible.<sup>3</sup>

The figures presented in the previous section already give us some idea about what can be the optimal energies and baseline for hierarchy and  $\delta_{CP}$  for  $\sin^2\theta_{13}$  in the above range.

If  $\sin^2\theta_{13}$  is close to its present best fit, then the LENF setup considered in this paper can determine hierarchy irrespective of what is the true  $\delta_{CP}$  for baselines  $\geq 1000$  km, with a 2.5-year exposure with each of the polarities and  $5 \times 10^{21}$  useful muon decays, as shown in Fig. 3. If true  $\delta_{CP}$  is not too close to  $3\pi/2$ , then even baselines  $\geq 700$  km would be sufficient for this purpose. The task of  $\delta_{CP}$  determination will also be easier:  $\delta_{CP}$  in the range  $(0.2-0.8)\pi$  and  $(1.2-1.8)\pi$  can be determined at  $5\sigma$  for baselines of 500–2000 km for  $E_\mu$  in the range 5–7 GeV, as can be seen from Fig. 5.

We can then be more ambitious and try to optimize the setup in order to get a  $5\sigma$  determination of hierarchy and  $\delta_{CP}$  with the minimum exposure. This is shown in Fig. 8, where we take the range of  $\sin^2\theta_{13}$  to be  $[0.013, 0.028]$ , the  $1\sigma$  range given in Ref. [1] in the prior and then marginalized over  $\theta_{13}$ .

It is clear from the top panel of the Fig. 8 that for any parent muon energy, the baseline  $L \sim 2500$  km is the optimal one for the determination of mass hierarchy. As mentioned before, this is near the bimagic baseline indicated in Ref. [19]. For a baseline of 1500 or 3500 km, the exposure needed may be an order of magnitude larger, depending on the  $\delta_{CP}$  value.

The bottom panel of Fig. 8 shows that for any  $E_\mu$  a baseline  $\sim 1300$  km will show the best sensitivity for  $\delta_{CP}$  discovery for most of the true values of  $\delta_{CP}$ . However, the “bimagic baseline” 2540 km will have comparable sensitivity with an exposure  $\sim 1.5$ -times larger. If  $\delta_{CP}(\text{true})$  happens to be close to  $5\pi/4$ ,  $\sim 2500$  km may show a better sensitivity compared to 1300 km. Note that the exposure needed for  $\delta_{CP}$  discovery at  $5\sigma$  is typically one order of magnitude higher than that for hierarchy determination.

## VIII. SUMMARY AND CONCLUDING REMARKS

The neutrino mixing angle  $\theta_{13}$ , the  $CP$  violating phase  $\delta_{CP}$ , and the hierarchy of neutrino mass eigenstates are the three quantities whose measurements are crucial in order to complete and confirm our current picture of neutrino mixing and oscillations. The next generation of long-baseline neutrino experiments therefore justifiably consider these measurements as their primary goals.

In this paper, we go beyond the conventional beam experiments and try to optimize the setup for a low energy neutrino factory (LENF) where the energy of the parent

<sup>3</sup>Also, see the Note added at the end of this paper for comments on the recent Daya Bay [5] and RENO [6] results.

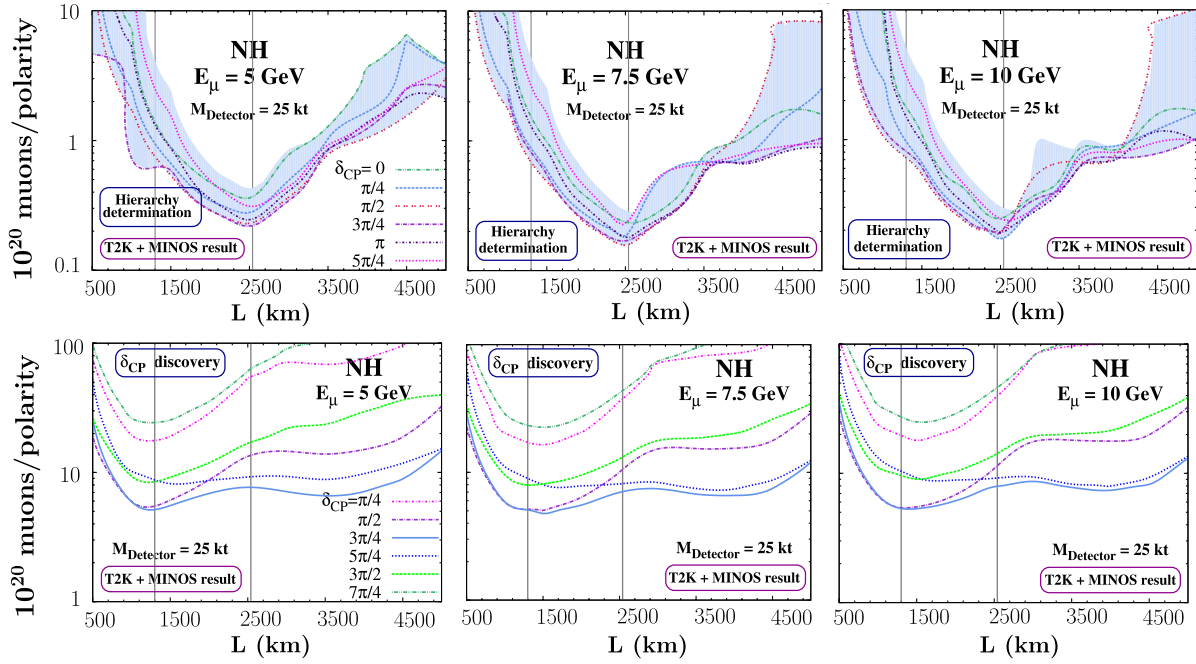


FIG. 8 (color online). Exposure required for  $5\sigma$  hierarchy determination (top panel) and  $\delta_{CP}$  discovery (bottom panel) if  $\theta_{13}$  is large. We have taken  $\sin^2\theta_{13} \in [0.013, 0.028]$  [1]. NH is taken as the true hierarchy, and all parameters except  $\delta_{CP}$  have been fixed at the values stated in Eq. (17).

muon is less than  $\sim 15$  GeV, and consider a magnetized totally active scintillator detector (TASD) that can identify neutrino muon charge for these measurements. In the worst-case scenario, i.e.,  $\theta_{13}$  turning out to be smaller than the reach of the current reactor and superbeam experiments, such setups can be used as discovery machines. On the other hand, if  $\theta_{13}$  is confirmed to be in the currently indicated range then one can use such machines for precision studies with the aim to measure the three quantities at the  $5\sigma$  level. In this paper we have focussed on the discovery potential.

We note that some of the parameters that determine the efficiency of a neutrino factory are beyond our control: the probability  $P_{e\mu}$  that controls this efficiency depends crucially on  $\theta_{13}$  and  $\delta_{CP}$ . However there are two parameters in our control: the baseline and the energy of the parent muon. It is with respect to these parameters that we perform our optimization.

It is of course obvious that the value of  $\theta_{13}$  would determine how efficient an experiment is. And that is true more or less in a straightforward way. In the absence of matter effects,  $P_{e\mu}$  is proportional to  $\theta_{13}^2$ . In the presence of matter effects,  $\theta_{13}$  affects the probability linearly, thus influencing the identification of mass hierarchy. The term in the probability that involves  $\delta_{CP}$  is also linear in  $\theta_{13}$ . Thus at shorter baselines (low matter effects), the value of  $\theta_{13}$  affects the measurement of  $\theta_{13}$  itself through a quadratic term, while at larger baselines, it affects the probability through a term that contains the product of itself with the matter effects.

In addition to  $\theta_{13}$ , we find that even the true value of  $\delta_{CP}$  can have a large impact on the reach of a LENF experiment. Indeed, the reach can change by up to an order of magnitude or more depending on the true value of  $\delta_{CP}$ . The actual value of  $|\Delta m_{31}^2|$  also affects the efficiency, albeit to a smaller extent. Given that the actual value of  $\delta_{CP}$  is crucial, we present our results in a way that bring out the impact of this parameter. We present three types of plots: (i) Type-A: plots in the  $\sin^2\theta_{13} - L$  plane for fixed values of  $|\Delta m_{31}^2|$  and  $\delta_{CP}$  varying in the range  $[0, 2\pi]$ , (ii) Type-B: plots in the  $\delta_{CP} - L$  plane for fixed values of  $\sin^2\theta_{13}$  and  $|\Delta m_{31}^2|$ , and (iii) Type-C: plots in the  $\sin^2\theta_{13} - L$  plane for fixed values of  $\delta_{CP}$  and varying  $|\Delta m_{31}^2|$  in its current  $3\sigma$  allowed range.

Most of the earlier work with the optimization of LENF presented the results in terms of “fraction of  $\delta_{CP}$ ” where the experiment was successful. However, it is crucial to know the exact range of  $\delta_{CP}$  where a certain measurement is possible, especially when one is thinking about combining results from two complementary experiments: these experiments should be sensitive to complementary ranges of  $\delta_{CP}$ .

Our detailed observations may be found in the main body of this text. We would like to attract the reader’s attention to some salient features. The following observations refer to 2.5 years of running with each muon polarity, with  $5 \times 10^{21}$  useful muon decays per year.

- (i) For  $\sin^2\theta_{13} \gtrsim 10^{-2}$ , mass hierarchy can be determined to  $5\sigma$  at almost all the baselines  $> 1000$  km.

For lower  $\theta_{13}$ , baselines  $\sim 2500$  km achieve the task for the largest fraction of  $\delta_{CP}$ ; however, even they may fall short when  $\delta_{CP}$  is near  $3\pi/2$ .

- (ii) Any baseline  $\leq 2000$  km can discover  $\theta_{13}$  if  $\sin^2\theta_{13} \gtrsim 10^{-3}$ . For smaller  $\theta_{13}$ , the choice of optimal baseline depends on the actual value of  $\delta_{CP}$ . However for majority of values of  $\delta_{CP}$ , the baseline range 1300–2500 km can be termed as optimal.
- (iii) The discovery of  $\delta_{CP}$  is naturally harder when its value is near 0 or  $\pi$ . However if  $\sin^2\theta_{13} \gtrsim 0.01$ , the discovery is possible for a wide range of  $\delta_{CP}$  values centered at  $\pi/2$  and  $3\pi/2$ . The range typically decreases with the increase of baseline.
- (iv) At a given baseline, when the parent muon energy is increased, the performance typically increases up to some energy and then remains the same. We term this as the saturation behavior.

As can be gathered from above, there does not exist a unique ‘‘optimal’’ baseline or muon energy for all performance indicators. The baseline determination depends, in addition to scientific merit, also on geography, economics, and sociology. Once that is determined, the optimization of muon energy involves mainly scientific and technical considerations. The saturation behavior mentioned above indicates that given a baseline, it is preferable to have the parent muon energy as close to the saturation energy as possible, in order to avoid increasing the parent muon energy unnecessarily. While the saturation energy may be determined through a detailed simulation for a given baseline (as we have done for three benchmark baselines in this paper), we have tried to come up with a simple criterion that can motivate this behavior and determine the saturation energy. We conjecture that the most efficient energy for a given baseline simply depends on the number of wrong-sign muons at the detector. This gives us a range of optimal muon energies for a given baseline, the range depending on the actual values of mixing parameters. This conjecture is vindicated *a posteriori* by the saturation energies obtained at the benchmark baselines. This simple-minded analysis gives an intuitive understanding of the relationship between baseline and the optimal energy.

With the recent indications of a large value of  $\theta_{13}$ , the  $5\sigma$  measurement of this quantity may already be within our grasp with the current experiments. Then the neutrino factory experiments have to aim higher, and the question to ask is what kind of setup will give us the  $5\sigma$  determination of mass hierarchy and  $CP$  violation with the least amount of exposure needed. Our analysis indicates that for the mass hierarchy, the baseline of  $\sim 2500$  km would perform the best at any parent muon energy. On the other hand, the measurement of  $CP$  violation is the most efficient around a baseline of  $\sim 1500$  km at all parent muon energies for most of the  $\delta_{CP}$  values.

A few comments are in order. We have presented all our results assuming the actual hierarchy to be NH. However,

note that the probabilities obtained with NH and  $\mu^+$  beam are identical with the probabilities with IH and  $\mu^-$  beam, and we have taken beams of both polarities with equal exposure. In LENF, both the polarities of muons can be accelerated at the same time, giving alternate bunches of  $\mu^+$  and  $\mu^-$ . The cross sections of  $\nu_\mu$  and  $\bar{\nu}_\mu$  on the nucleons are also virtually identical at the relevant energies, and hence our results are valid even for IH.

Another comment is about the measurement of  $\delta_{CP}$  itself. In this paper, we have only considered the discovery potential for  $CP$  violation, i.e., we are interested in finding a nonzero  $\delta_{CP}$ . This task is, naturally, hard for small  $\delta_{CP}$  and impossible when  $\delta_{CP} = 0$  or  $\pi$ . However with large  $\theta_{13}$ , a measurement of  $\delta_{CP}$  may be possible even if its value is close to the  $CP$ -conserving limit. If indeed the value of  $\theta_{13}$  is confirmed to be large, one can aim to answer more detailed questions like the value of  $\delta_{CP}$ , the octant of  $\theta_{23}$ , or the deviation of  $\theta_{23}$  from maximality. These quantities will not be analyzed in this work.

Finally, the most important quantity is the one we have no control over: the value of  $\theta_{13}$ . As far as neutrino factories are concerned, this quantity will determine if they are going to be discovery machines or precision machines.

## ACKNOWLEDGMENTS

We thank S. Prakash, S. Raut, and S. Uma Sankar for useful discussions. S.R. would like to thank Yuval Grossman for support and hospitality.

*Note added.*—While this paper was under review, new results were announced by the Daya Bay [5] and RENO [6] experiments which claimed the discovery of a nonzero  $\theta_{13}$  to more than  $5\sigma$ . Indeed the Daya Bay measurement gives  $\sin^2\theta_{13} = 0.023 \pm 0.004 \pm 0.001$ , while the RENO experiment gives  $\sin^2\theta_{13} = 0.026 \pm 0.004 \pm 0.004$ . The analysis in this paper has been done assuming that the value of  $\theta_{13}$  is still unknown; however, it stays valid even with a measured nonzero value. (Of course, the results about  $\theta_{13}$  discovery would become redundant.) Indeed, the projections for the reach of the LENF would become even more optimistic, and the results in Sec. VII gain even more significance. The range of  $\sin^2\theta_{13}$  taken in the analysis in Sec. VII is (0.013, 0.028) which overlaps with the  $1\sigma$  range of the Daya Bay and RENO measurements. The results in Fig. 8 then indicate that the baseline of  $\sim 2500$  km can yield the mass hierarchy with the minimum amount of exposure, while the baseline  $\sim 1500$  km would be the optimal for the detection of nonzero  $\delta_{CP}$ . Note that with the value of  $\theta_{13}$  as large as that measured by these experiment, the measurement of  $CP$  violation at the LENF would be a real possibility. With a detector capable of distinguishing  $\mu^+$  from  $\mu^-$  (and hence,  $\nu_\mu$  from  $\bar{\nu}_\mu$ ), a LENF would then become the front runner in the race for the first observation of  $CP$  violation in the lepton sector.

- [1] G.L. Fogli, E. Lisi, A. Marrone, A. Palazzo, and A. M. Rotunno, *Phys. Rev. D* **84**, 053007 (2011).
- [2] T. Schwetz, M. Tortola, and J. W. F. Valle, *New J. Phys.* **13**, 109401 (2011).
- [3] K. Abe *et al.* (T2K Collaboration), *Phys. Rev. Lett.* **107**, 041801 (2011).
- [4] L. Whitehead (MINOS Collaboration), in Recent Results from MINOS, [http://www.numi.fnal.gov/pr\\_plots/](http://www.numi.fnal.gov/pr_plots/).
- [5] F.P. An *et al.* (DAYA-BAY Collaboration), *Phys. Rev. Lett.* **108**, 171803 (2012).
- [6] J.K. Ahn *et al.* (RENO Collaboration), *Phys. Rev. Lett.* **108**, 191802 (2012).
- [7] A. de Gouvea, J. Jenkins, and B. Kayser, *Phys. Rev. D* **71**, 113009 (2005); A. de Gouvea and W. Winter, *Phys. Rev. D* **73**, 033003 (2006); R. Gandhi, P. Ghoshal, S. Goswami, and S. U. Sankar, *Mod. Phys. Lett. A* **25**, 2255 (2010).
- [8] F. Ardellier *et al.*, [arXiv:hep-ex/0405032](https://arxiv.org/abs/hep-ex/0405032); X. Guo *et al.* (Daya-Bay Collaboration), [arXiv:hep-ex/0701029](https://arxiv.org/abs/hep-ex/0701029); J. K. Ahn *et al.* (RENO Collaboration), [arXiv:1003.1391](https://arxiv.org/abs/1003.1391).
- [9] D. Indumathi and M. V. N. Murthy, *Phys. Rev. D* **71**, 013001 (2005); R. Gandhi, P. Ghoshal, S. Goswami, P. Mehta, and S. Uma Sankar, *Phys. Rev. D* **73**, 053001 (2006); S. T. Petcov and T. Schwetz, *Nucl. Phys.* **B740**, 1 (2006); R. Gandhi, P. Ghoshal, S. Goswami, P. Mehta, S. U. Sankar, and S. Shalgar, *Phys. Rev. D* **76**, 073012 (2007); A. Samanta, *Phys. Lett. B* **673**, 37 (2009).
- [10] P. Huber, M. Lindner, T. Schwetz, and W. Winter, *J. High Energy Phys.* **11** (2009) 044.
- [11] A. Bandyopadhyay *et al.* (ISS Physics Working Group Collaboration), *Rep. Prog. Phys.* **72**, 106201 (2009).
- [12] V. Barger, D. Marfatia, and K. Whisnant, *Phys. Rev. D* **65**, 073023 (2002); P. Huber and W. Winter, *Phys. Rev. D* **68**, 037301 (2003).
- [13] K. Long, Proc. Sci., ICHEP2010 (2010) 521.
- [14] S. Geer, O. Mena, and S. Pascoli, *Phys. Rev. D* **75**, 093001 (2007);
- [15] E. Fernandez Martinez, T. Li, S. Pascoli, and O. Mena, *Phys. Rev. D* **81**, 073010 (2010).
- [16] S. K. Agarwalla, P. Huber, J. Tang, and W. Winter, *J. High Energy Phys.* **01** (2011) 120.
- [17] P. Huber and T. Schwetz, *Phys. Lett. B* **669**, 294 (2008).
- [18] S. K. Raut, R. S. Singh, and S. U. Sankar, *Phys. Lett. B* **696**, 227 (2011).
- [19] A. Dighe, S. Goswami, and S. Ray, *Phys. Rev. Lett.* **105**, 261802 (2010).
- [20] M. V. Diwan *et al.*, *Phys. Rev. D* **68**, 012002 (2003).
- [21] J. Peltoniemi, [arXiv:0911.4876](https://arxiv.org/abs/0911.4876).
- [22] A. Joglekar, S. Prakash, S. K. Raut, and S. U. Sankar, *Mod. Phys. Lett. A* **26**, 2051 (2011); S. K. Agarwalla, T. Li, and A. Rubbia, *J. High Energy Phys.* **05** (2012) 154.
- [23] A. Y. Smirnov, [arXiv:hep-ph/0610198](https://arxiv.org/abs/hep-ph/0610198).
- [24] E. K. Akhmedov, R. Johansson, M. Lindner, T. Ohlsson, and T. Schwetz, *J. High Energy Phys.* **04** (2004) 078.
- [25] J. Burguet-Castell, M. B. Gavela, J. J. Gomez-Cadenas, P. Hernandez, and O. Mena, *Nucl. Phys.* **B608**, 301 (2001); H. Minakata and H. Nunokawa, *J. High Energy Phys.* **10** (2001) 001.
- [26] G.L. Fogli and E. Lisi, *Phys. Rev. D* **54**, 3667 (1996).
- [27] A. M. Dziewonski and D. L. Anderson, *Phys. Earth Planet. Inter.* **25**, 297 (1981).
- [28] P. Huber and T. Schwetz, *Phys. Lett. B* **669**, 294 (2008).
- [29] P. Huber, M. Lindner, and W. Winter, *Comput. Phys. Commun.* **167**, 195 (2005); P. Huber, J. Kopp, M. Lindner, M. Rolinec, and W. Winter, *Comput. Phys. Commun.* **177**, 432 (2007).